

Diffractionless beam in free space with adiabatic changing refractive index in a single mode tapered slab waveguide

Chang-Ching Tsai^{*}, Claudio Vinegoni² and Ralph Weissleder³

Center for Systems Biology, Massachusetts General Hospital and Harvard Medical School
Boston, Massachusetts 02114

[*Tsai.Chang-Ching@mgh.harvard.edu](mailto:Tsai.Chang-Ching@mgh.harvard.edu)

Abstract: We propose a novel design to produce a free space diffractionless beam by adiabatically reducing the difference of the refractive index between the core and the cladding regions of a single mode tapered slab waveguide. To ensure only one propagating eigenmode in the adiabatic transition, the correlation of the waveguide core width and the refractive index is investigated. Under the adiabatic condition, we demonstrate that our waveguide can emit a diffractionless beam in free space up to 500 micrometers maintaining 72% of its original peak intensity. The proposed waveguide could find excellent applications for imaging purposes where an extended depth of field is required.

©2009 Optical Society of America

OCIS codes: (230.7400) Waveguides, slab; (050.1970) Diffractive optics; (130.0130) Integrated optics

References and links

1. P. J. Verveer, J. Swoger, F. Pampaloni, K. Greger, M. Marcello and E. H. K. Stelzer, "High-resolution three dimensional imaging of large specimens with light sheet-based microscopy," *Nat. Methods* **4**, 311-313 (2007).
2. Z. Ding, H. Ren, Y. Zhao, J. S. Nelson, and Z. Chen, "High-resolution optical coherence tomography over a large depth range with an axicon lens," *Opt Lett.* **27**, 243-245 (2002).
3. G. Miękula, Z. Jaroszewicz, A. Kolodziejczyk, K. Petelczyc and M. Sypek, "Imaging with extended focal depth by means of lenses with radial and angular modulation," *Opt. Express* **15**, 9184-9193 (2007).
4. J. A. García, S. Bará, M. G. García, Z. Jaroszewicz, A. Kolodziejczyk, and K. Petelczyc, "Imaging with extended focal depth by means of the refractive light sword optical element," *Opt. Express* **16**, 18371-18378 (2008).
5. B.-Z. Dong, J. Liu, B.-Y. Gu, and G.-Z. Yang, "Rigorous electromagnetic analysis of a microcylindrical axilens with long focal depth and high transverse resolution," *J. Opt. Soc. Am. A* **18**, 1465-1470 (2001).
6. E. R. Dowski, Jr. and W. T. Cathey, "Extended depth of field through wave-front coding," *Appl. Opt.* **34**, 1859-1866 (1995).
7. J. G. Ritter, R. Veith, J.-P. Siebrasse and U. Kubitschek, "High-contrast single-particle tracking by selective focal plane illumination microscopy," *Opt. Express* **16**, 7142-7152 (2008).
8. D.-Z. Lin, C.-H. Chen, C.-K. Chang, T.-D. Cheng, C.-S. Yeh, and C.-K. Lee, "Subwavelength nondiffraction beam generated by a plasmonic lens," *Appl. Phys. Lett.* **92**, 233106-1-3 (2008).
9. J. Ojeda-Castañeda, E. Tepichin, and A. Diaz, "Zone plate for arbitrarily high focal depth," *Appl. Opt.* **29**, 994-997 (1990).
10. R. Arimoto, C. Saloma, T. Tanaka, and S. Kawata, "Imaging properties of axicon in a scanning optical system," *Appl. Opt.* **31**, 6653-6657 (1992).
11. J. Arlt, V. Garces-Chavez, W. Sibbett, K. Dholakia, "Optical micromanipulation using a Bessel light beam," *Opt. Commun.* **197**, 239-245 (2001).
12. A. J. Cox and D. C. Dibble, "Nondiffracting beam from a spatially filtered Fabry-Perot resonator," *J. Opt. Soc. Am. A* **9**, 282-286 (1992).
13. Jari Turunen, Antti Vasara, and Ari T. Friberg, "Holographic generation of diffraction-free beams," *Appl. Opt.* **27**, 3959-3962 (1988).

14. J. H. McLeod, "The Axicon: A New Type of Optical Element," *J. Opt. Soc. Am.* **44**, 592-597 (1954)
 15. J. Durnin, "Exact solutions for nondiffracting beams. I. The scalar theory," *J. Opt. Soc. Am. A* **4**, 651-654 (1987).
 16. Y. Shani, C. H. Henry, R. C. Kistler, K. J. Orlowsky, and D. A. Ackerman, "Efficient coupling of a semiconductor laser to an optical fiber by means of a tapered waveguide on silicon," *Appl. Phys. Lett.* **55**, 2389-2391 (1989).
 17. Y. Xu, R. K. Lee, and A. Yariv, "Adiabatic coupling between conventional dielectric waveguides and waveguides with discrete translational symmetry," *Opt. Lett.* **25**, 755-757 (2000).
 18. C.-C. Tsai, L. B. Glebov, and B. Ya. Zeldovich, "Adiabatic three-wave volume hologram: large efficiency independent of grating strength and polarization," *Opt. Lett.* **31**, 718-720 (2006)
 19. J. Gerdes and R. Pregla, "Beam-propagation algorithm based on the method of lines," *J. Opt. Soc. Am. B* **8**, 389-394 (1991).
 20. J. J. Gerdes, "Bidirectional eigenmode propagation analysis of optical waveguides based on method of lines," *Electron. Lett.* **30**, 550-551 (1994).
 21. S. J. Al-Bader and H. A. Jamid, "Perfectly matched layer absorbing boundary conditions for the method of lines modelling scheme," *IEEE Microwave Guided Wave Lett.* **8**, 357-359 (1998)
 22. J. Gerdes, B. Lunitz, D. Benish and R. Pregla, "Analysis of slab waveguide discontinuities including radiation and absorption effects," *Electron. Lett.* **28**, 1013-1015 (1992).
 23. M. Imtaar and S. J. Al-Bader, "Analysis of diffraction from abruptly terminated optical fibers by the method of lines," *J. Lightwave Technol.* **13**, 137-141 (1995).
 24. M. G. Moharam, D. A. Pommet, and E. B. Grann, T. K. Gaylord, "Stable implementation of the rigorous coupled-wave analysis for surface-relief gratings: enhanced transmittance matrix approach," *J. Opt. Soc. Am. A* **12**, 1077-1086 (1995).
 25. J. Hecht, *Understanding Fiber Optics*, (Prentice Hall, 2006).
-

1. Introduction

Diffractionless beams with large depth of focus (DOF) have significant applications in three dimensional biomedical imaging, such as optical coherence tomography (OCT) and single plane illumination microscopy (SPIM) [1-2]. For two dimensional imaging, the image resolution in the transverse plane (x - y) is determined by the beam size $r(x,y)$ on the focal plane at the distance z . For three dimensional imaging, to keep the same image resolution in a light propagation interval Δz inside the sample, an invariant beam size along the z -axis is required. In other words, the longitudinal image resolution is limited by the DOF of the beam.

Many efforts have been made so far to increase the DOF in different optical systems. Most of the techniques focus on modulating the phase transmission function over the lens [3-5], or the wavefronts coding [6]. The use of cylindrical or plasmonic lenses can provide high image resolution, but their DOFs are not large enough for deep bio-medical imaging [7-8]. Optical power-absorbing apodizers can offer larger DOF, but the drawback of losing the incident energy alternately reduces the image resolution and can be only applied to strong illumination sources [9]. Typically, the diffractionless Bessel beams produced by axicons or Fabry-Perot interferometers or holograms [10-13] are often employed to complete the task.

In this paper, we propose a novel way to generate a diffraction limited beam by varying the refractive index adiabatically in a tapered-wave guide. Our method features a very simple and tiny structure, which can be directly applied to, for example, SPIM as illustrated in Fig. 1. Simulations demonstrate that the proposed design achieves a high diffractionless beam with propagation distance up to 500 μm , while maintaining 72% of its original peak power without any micro-lens attached. We will first address the theoretical background of eliminating diffraction by reducing the index difference in the equivalent phase aperture. Next we will consider the condition of producing such diffractionless beam by adiabatic transition of eigenmodes in a slab symmetric waveguide and numerical results will be provided. Finally we will discuss potential applications and extensions of our work.

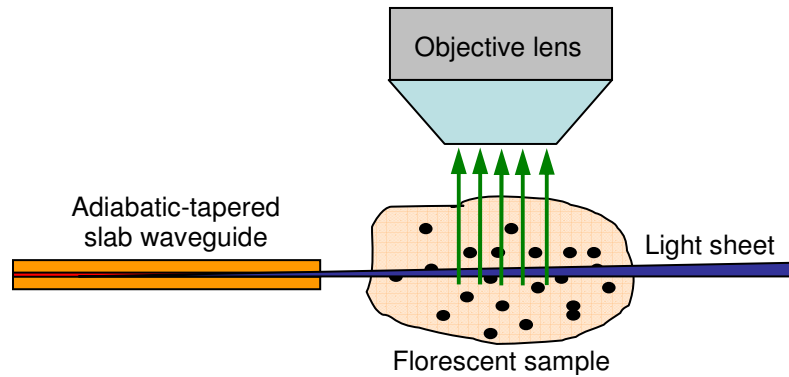


Fig. 1. The application of non-diffracted beam emitted from adiabatic tapered-waveguide to single plane illumination microscopy (SPIM).

2. Theoretical background and principle of design

Limited aperture sizes and finite wavelengths are the causes of diffraction as described by the Huygens-Fresnel principle. The Airy pattern of light diffracted by a circular aperture of diameter D in the Fraunhofer region gives diffraction a quantitative description in terms of the wavelength and aperture size. By inspecting its first zero radius $J_1(x) \approx 1.22 f\lambda/D$, it indicates that the beam spreads out severely if the aperture is sufficiently small compared with the wavelength λ . However as pointed out by McLeod [14], a ring aperture can form a line of image without severe diffraction. This is later labeled as Bessel beam, which is indeed a non-diffracted solution of the Helmholtz wave equation [15]. Basically, Bessel beams are light of ring-patterns originally due to either the Fourier spectrum of an annular slit or the conical lens of virtual ring structure in the far field [14] and it can be considered as the earliest scheme of modulating the phase transmission function on the aperture to produce diffractionless beam. Most of the other schemes today basically follow the manipulation of the phase transmission function on different optical elements. In this paper, we turn our attention out of the Fourier diffraction and seek for alternative approaches.

Let us first consider the beam inside a waveguide, which is the optical mode that satisfies the boundary condition of Maxwell equations in bounded space. The wave propagating inside the waveguide is confined in the small core region, so the lateral beam size is about the same order of the core width. In a natural way, the waveguide generates a continuous small size beam without the concept of focusing. However, this property is only supported inside the waveguide. Due to the small core width and the discontinuity of the refractive index in the facets of waveguides or optical fibers, the beams suffer severe divergence when emitted out in free space. The challenge then is to find a way to let the beam pass smoothly through the facet with the minimum of diffraction. For simplicity, we are particularly interested in investigating the single-mode waveguide, since the multi-modes will create more complicated beam profile in the transverse plane. Furthermore, we will discuss the symmetric waveguide with examples of TE polarized wave only.

Disregarding the nature of the mode in the waveguide, the core sandwiched in the substrate and cladding at the end of a waveguide is analog to the phase aperture in the Fresnel-Kirchhoff diffraction theory. Hence, if we let the core refractive index n_c infinitesimally approach that of the substrate n_s (the same refractive index in cladding), the phase aperture essentially diminishes. In this way, we would expect the output beam to be diffractionless. In this extreme condition ($n_c \rightarrow n_s$), we should first explore the possibility of the existence of a single propagating mode. The propagating mode is decided by the wave incident angle on the boundary of the waveguide, which should be larger than the critical angle $\theta_c = \sin^{-1}(n_s/n_c)$. In our diminishing case, if $n_c \rightarrow n_s$, then $\theta_c \rightarrow 90^\circ$. For this situation, the propagating mode

exists as long as $n_c > n_s$ and its existence can be proved from the analytical solution of the slab waveguide. We will label this type of waveguide as “grazing waveguide,” accounting for the fact that the incident angle of the ray bouncing inside the waveguide is nearly 90° , i.e. almost tangent to the boundary.

To demonstrate that the diminishing of the refractive index difference can lead to a diffractionless beam, in Figs. 2(a) and 2(b) we compare the numerical results of the output intensities from a single-mode waveguide and the “grazing waveguide” respectively. These two waveguides have the same configurations and parameters except for the refractive index value n_c within the core region. In Fig. 2(a) we choose $n_s = 1.48$, and $n_c = 1.5$ while we let $n_c = 1.4801$ in Fig. 2(b). Comparing the two sets of the transverse beam intensities at $z = 0, 10, 20, 50, 100 \mu\text{m}$ in Figs. 2(c) and 2(d), it is clear that the grazing waveguide generates a less diffractive beam, which keeps above 92% of the original peak power. However, for such low contrast of refractive index, the beam size broadens a lot as the FWHM inside the waveguide increases from $0.70 \mu\text{m}$ in Fig. 2(c) to $18.81 \mu\text{m}$ in Fig. 2(d). On the other side increasing the core width w in the grazing waveguide can help reducing the beam size as clearly shown in Fig. 3(b). In this case, the FWHM is reduced to $7.38 \mu\text{m}$ with $w = 5.4 \mu\text{m}$ while keeping the same parameters as in Fig. 2(b).

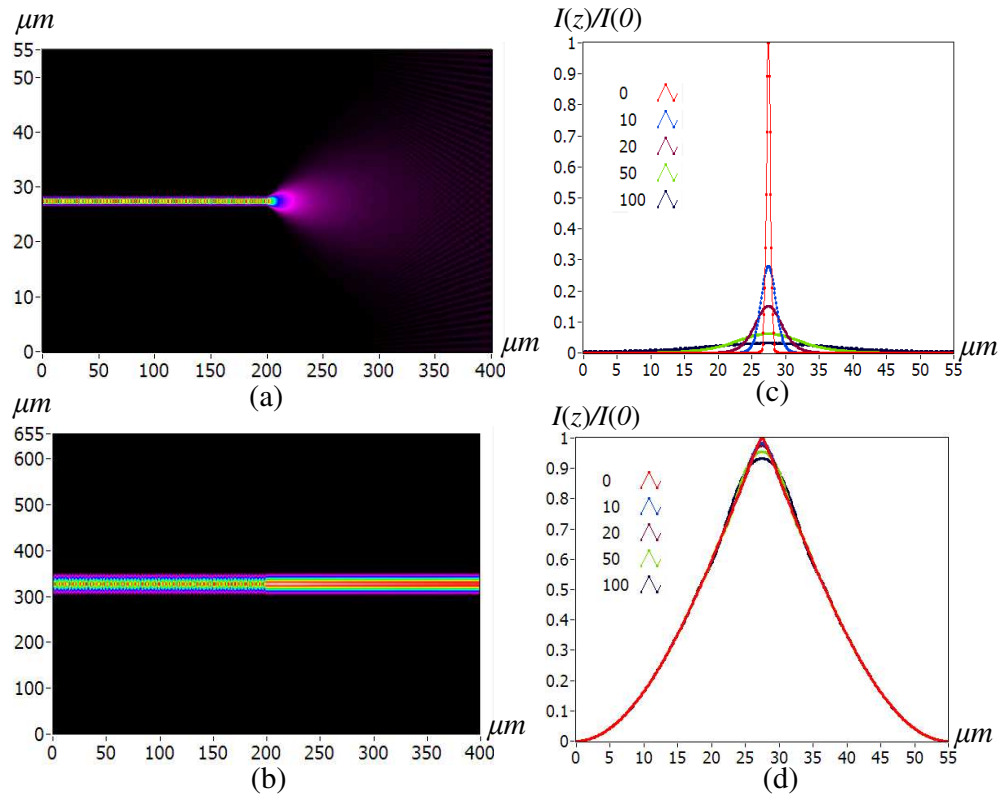


Fig. 2. (a). Divergence of beam emitting from a single-mode symmetric slab waveguide into air with incident wavelength $\lambda = 0.405 \mu\text{m}$, core width $w = 0.8 \mu\text{m}$, core refractive index $n_c = 1.5$ and substrate $n_s = 1.48$. The waveguide length is $200 \mu\text{m}$ and the propagation distance in air is also $200 \mu\text{m}$. (b). Diffractionless beam coming out from the grazing waveguide with the same configuration as in (a) except the core refractive index $n_c = 1.4801$. (c) Transverse beam profiles of (a) in the air at $z = 0, 10, 20, 50, 100 \mu\text{m}$ respectively with intensity $I(z)/I(0)$ normalized to 1 at $z = 0$. (d) Transverse beam profiles of (b) $I(z)/I(0)$ up to propagating distance $100 \mu\text{m}$ in air with almost constant FWHM = $18.81 \mu\text{m}$.

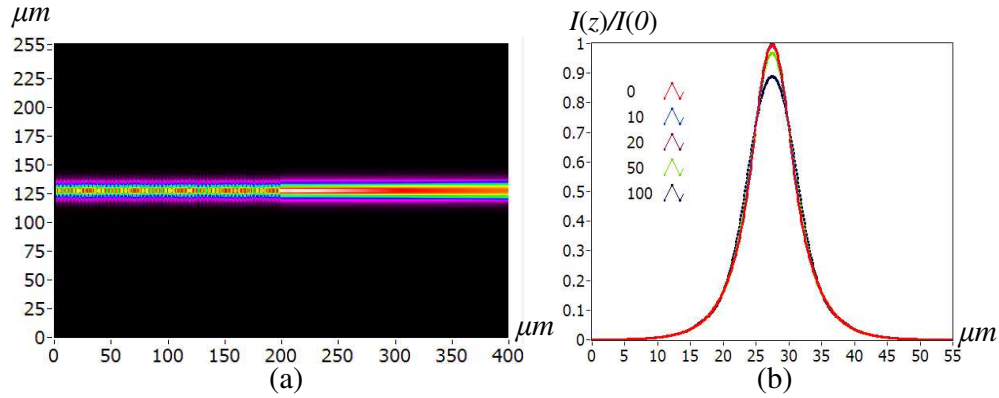


Fig. 3 (a). Diffractionless beam emitting from the grazing waveguide with the same condition as in Fig. 1 (b) but with an increased core width $w = 5.4 \mu\text{m}$. (b) Transverse beam profiles of (a) $I(z)/I(0)$ at $z = 0, 10, 20, 50, 100 \mu\text{m}$ in air with almost constant FWHM = $7.38 \mu\text{m}$.

Although we have numerically demonstrated that the grazing waveguide can produce a diffractionless beam, in reality it is quite a challenge to launch such a grazing mode. Normally, the coupling loss increases with decreasing the waveguide's numerical aperture (NA). This loss is particularly severe for the grazing waveguide case due to the extremely small NA ($NA = [n_c^2 - n_s^2]^{0.5} \rightarrow 0$). Therefore, our next task is to find a solution to generate the grazing mode, which is the other part in our research.

It is known in many physical systems with operators of different eigen-problems, that if the operator changes slowly (with time or distance or both) the corresponding eigenmode can transform into the other without losing the characteristics of mode. This is known as the principle of adiabatic mode transition. Generally, the condition of adiabatic condition can be written as $|\partial \mathbf{f} / \partial \mathbf{x}| \ll \mathbf{f}$, where \mathbf{f} is the vector of mode-characterized parameters and \mathbf{x} is a vector of dimensionless variables either in time- or space-domain or both. In optics the adiabatic transitions of optical modes are typically made by variation of the material properties or the geometrical structure. This concept has been applied to waveguide-fiber couplers, slab-photonic crystal waveguides coupling, and volume holograms [16-18].

We utilized the adiabatic mode-evolution to change the propagating mode in a high divergent waveguide to a diffractionless mode in a grazing waveguide. Here the Helmholtz wave equation inside the waveguide can be written as,

$$\frac{d^2 E}{dz^2} + (n^2(z) - n_{eff}^2 k_0^2) E = 0 \quad (1),$$

where n_{eff} is the effective refractive index. For a single-mode symmetric waveguide the $n_{eff}(n, w)$, the refractive index $n(z)$, and the core width $w(z)$ are related as,

$$n_{eff} = \sqrt{\left(\frac{\gamma_{c,s}}{k_0}\right)^2 + n_{c,s}^2(z)}, \quad \gamma_c = \frac{1}{w(z)} \left\{ -2 \tan^{-1}\left(\frac{\gamma_c}{\gamma_s}\right) + \pi \right\} \quad (2),$$

where $\gamma_{c,s}$ are the transverse propagation constants in the core and substrate region respectively. The adiabatic transition criterion can then be here expressed as

$$\frac{1}{n_{eff} k_0} \left| \frac{dn_{eff}}{dz} \right| \ll n_{eff}(n, w) \quad (3).$$

Here we emphasize that it is nontrivial to select the right adiabatic process in order to achieve a diffractionless beam. In fact to produce a high quality beam and prevent several propagating modes mixing up, we should manage the core size and its refractive index to remain a single-mode waveguide during the adiabatic following process at all times. This is essential. Mathematically, if we assume that all the eigen-vectors of the Helmholtz operator of the waveguide constitute a complete set in Hilbert space, then the space spanned in a single-mode waveguide allows only one eigenvector with real eigenvalue (propagating mode). But for multi-mode waveguides there are more than one such eigenvectors. Hence, an eigenmode in single-mode waveguide propagating into multi-mode waveguide will project itself onto several propagating modes with non-zero components. This will cause the rising of multi-propagating-modes during the beam propagation. Therefore, the adiabatic tapered-waveguide must be designed in such a way that in any segment of the waveguide there is always only one propagating mode. If this condition is not satisfied the beam profile will become complicated due to the mixing up at each propagating stage, and it will lead to a high divergent beam at the end of the waveguide as obtained from our numerical experiment. Fig. 3(a) shows the adiabatic condition of tuning the core width $w(z)$ and the refractive index $n_c(z)$ with respect to the propagation distance z in a single-mode grazing waveguide. Here the ideal continuously varying parameters $w(z)$ and $n_c(z)$ along z are modeled by the stair-case approximation [19], with each segment $\Delta L = 2000 \mu\text{m}$ for a total waveguide length $L = 46000 \mu\text{m}$ (23 partitions). Fig. 4(b) shows the values of $n_{\text{eff}}(n, w)$ and $dn_{\text{eff}}/(n_{\text{eff}} k_0) dz$ that satisfy Eq.(3) along the parametric curve of Fig. 4(a). Following this adiabatic condition we will show in the next section the numerical results of the beam propagating in free space.

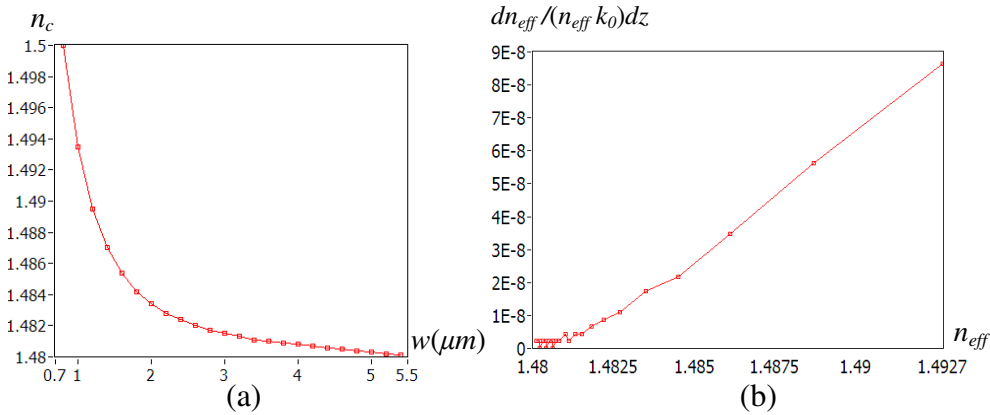


Fig. 4. (a). The adiabatic condition for transforming the lowest eigenmode with $\lambda = 0.405 \mu\text{m}$ in a single-mode waveguide with $w = 0.8 \mu\text{m}$, $n_c = 1.5$, $n_s = 1.48$ into the diffractionless mode in the grazing waveguide with $w = 5.4 \mu\text{m}$, $n_c = 1.4801$, $n_s = 1.48$. The core refractive index $n_c(z)$ and width $w(z)$ are kept at constant value within every segment i with $\Delta L = 2000 \mu\text{m}$ in the stair-case approximation of $46000 \mu\text{m}$ in 23 stairs. (b) Curve of effective refractive index n_{eff} and $dn_{\text{eff}}/(n_{\text{eff}} k_0) dz$ obtained from Eq.(2) and (3), according to the parameters in (a).

3. Numerical results of the diffractionless grazing waveguide

For our simulations we use the Method of Line-Beam Propagation Method (MoL-BPM) [19-20] with perfect matched layer (PML) boundary condition [21]. This method has been demonstrated to give accurate results for beams propagating inside a multi-junctions waveguide and into free space from abrupt-terminated waveguide facet including radiation and absorption effects [22-23]. We modeled the continuously changing waveguide profile by stair-case approximation. To avoid the numerical overflow during the eigen-matrices iterating and inverting processes we used Enhanced Transmittance Matrix Approach (ETMA) to do the

computation [24]. Theoretically, in a smoothly adiabatic process there is no reflection during the eigenmode transformation. In the stair-case approximation, there is a negligible amount of reflection at each interface of segment. Numerical experiments show that the total reflectivity is almost the same as the light emitted from a normal single waveguide into the air. Following the parameter curve of Fig. 4(a) we design the appropriate waveguide structure for the diffractionless beam in Fig. 5(a). The simulation condition is that we started from the lowest eigenmode in a slab waveguide with $\lambda = 0.405 \mu\text{m}$, $w = 0.8 \mu\text{m}$, $n_c = 1.5$, $n_s = 1.48$ and transform it into the diffractionless mode in the grazing waveguide with $w = 5.4 \mu\text{m}$, $n_c = 1.4801$, $n_s = 1.48$. In stair-case approximation, the core refractive index $n_c(z)$ and width $w(z)$ are kept at constant value within each stair i of $\Delta L = 2000 \mu\text{m}$ in a total length $L = 46000 \mu\text{m}$ with 23 partitions. The beam intensities inside the waveguide as well as in the air are calculated and shown in Figs. 5(b) and 5(c) respectively. Fig. 5(d) gives the transverse beam profile at different propagation distance $z = 0, 10, 20, 50, 100, 150, 200, 250 \mu\text{m}$ in the air. We see that Fig. 5(d) depicts similar non-diffraction feature at $z = 0, 10, 20, 50, 100 \mu\text{m}$ as in Fig. 3(b) after the adiabatic transition. The non-diffracted quality of the beam can be determined by examining the peak intensities and the FWHMs of the above beam profiles. By setting the peak value equal to 1 at $z = 0 \mu\text{m}$ (calculated FWHM = $7.41 \mu\text{m}$), we obtain at $z = 100 \mu\text{m}$ a peak value of 0.901 with a FWHM = $8.95 \mu\text{m}$. After propagating $100 \mu\text{m}$ in free space, the peak still keeps 90% of its value and the FWHM broadens only 20%. The grazing waveguide indeed can emit a high diffractionless beam without any external lens attached. At large distance $z = 250 \mu\text{m}$, the peak value is 0.728, which keeps 72% of the initial intensity at $z = 0$. This demonstrates the feasibility of efficient light coupling into the diffractionless grazing waveguide by stair-case transition.

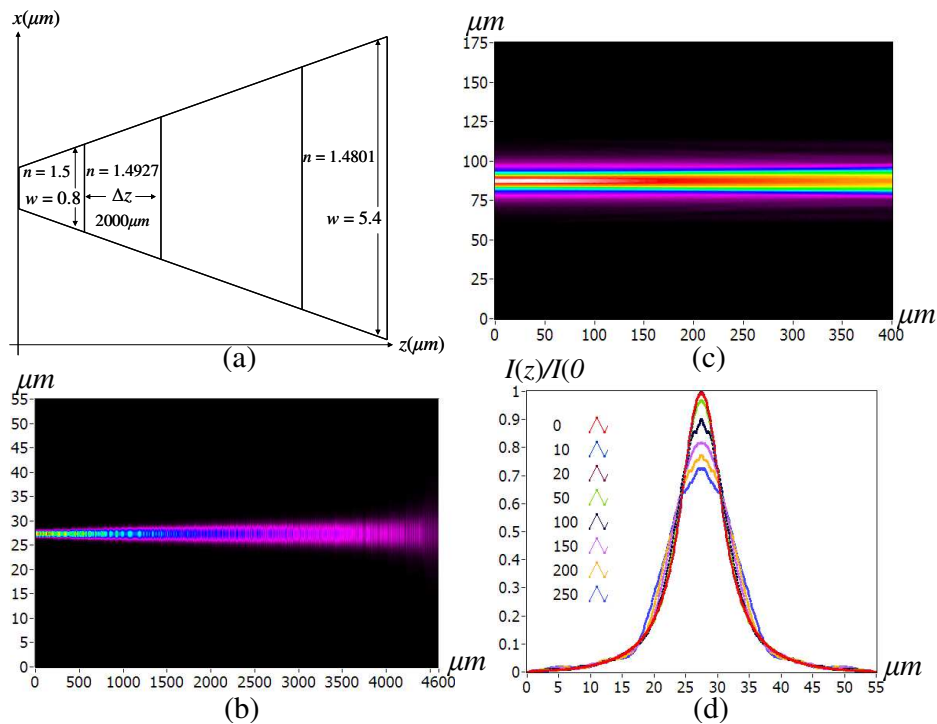


Fig. 5. (a) Side view of the adiabatic-grazing slab waveguide, with the configuration according to Fig. 3(a). (b) Intensities of TE wave inside the waveguide before emitting out. (c) Intensities of beam propagating in air after emitting out. (d) The transverse profiles (cross sections) of the beam in (c) at $z = 0, 10, 20, 50, 100, 150, 200,$ and $250 \mu\text{m}$ respectively, with intensities $I(z)/I(0)$ normalized at $z = 0$.

Since there is no cut-off condition for the lowest mode in a symmetric slab waveguide, we further check the transition of propagating mode for the effective refractive index n_{eff} very close to the refractive index of cladding n_c in a shorter partition length ΔL in the following.

Based on the adiabatic condition Eq. (3) and the waveguide structure of Fig. 5(a), we investigate the diffractionless property of the grazing waveguide by reducing the core refractive index n_c another numerical order to 1.48001. This time we divide the waveguide into 56 slices with each partition $\Delta L = 200 \mu\text{m}$. The parametric curve of the waveguide configuration $n_c(\Delta L)$ and $w(\Delta L)$ is plotted in Fig. 6(a). We show the results of the beam propagation in the waveguide and air in Fig. 6(b) and 6(c) respectively. Fig. 6(d) gives the cross sections of the intensity distribution of the beam of Fig. 6(c) at distance $z = 0, 100, 200, 300, 400,$ and $500 \mu\text{m}$. Data clearly indicate that the peak of the beam keeps the value above 0.983 in the first $100 \mu\text{m}$ with FWHM = $14 \mu\text{m}$. Then it reduces to 0.88 at $z = 200 \mu\text{m}$ with FWHM = $15.95 \mu\text{m}$. At $z = 500 \mu\text{m}$, the peak intensity is 0.723, i.e. 72% of its value after emitting with a beam size with FWHM = $20.8 \mu\text{m}$.

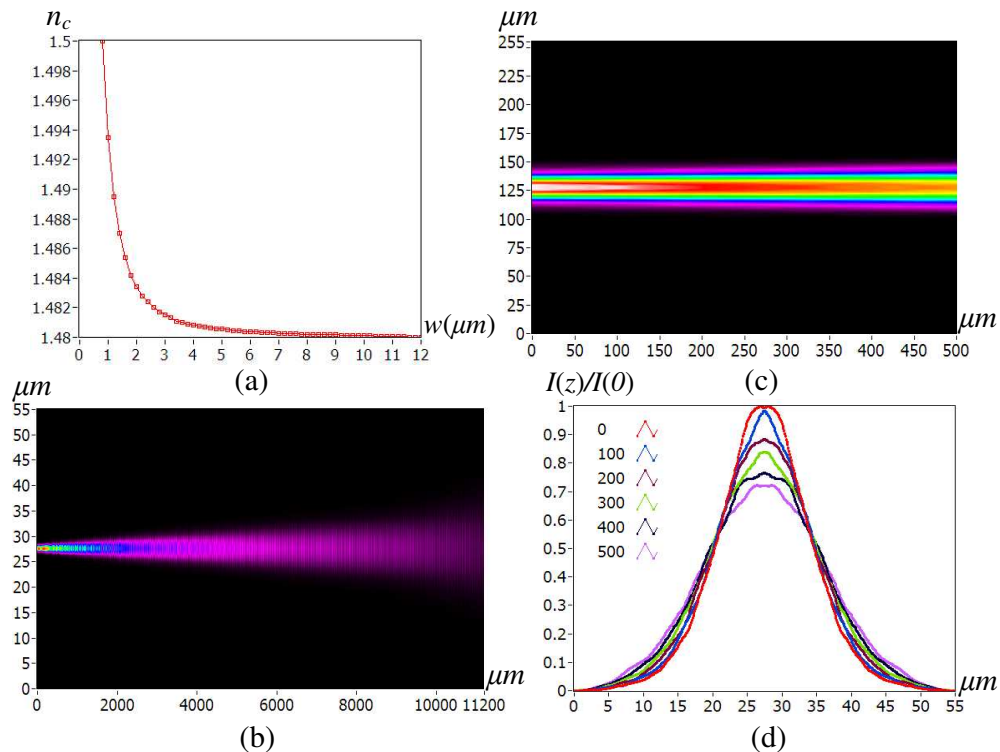


Fig. 6. (a) The adiabatic condition for transforming a eigenmode with $\lambda = 0.405 \mu\text{m}$ in a single-mode waveguide with $w = 0.8 \mu\text{m}$, $n_c = 1.5$, $n_s = 1.48$ into the diffractionless mode in the grazing waveguide with $w = 12 \mu\text{m}$, $n_c = 1.48001$, $n_s = 1.48$. The core refractive index $n_c(z)$ and width w (z) are kept at constant value within every segment i with $\Delta L = 200 \mu\text{m}$ in the stair-case approximation of $11200 \mu\text{m}$ in 56 partitions. (b) Intensities of TE wave inside the waveguide before emitting out. (c) Intensities of beam propagating in the air after emitting out. (d) Transverse profiles (cross sections) of the beam in (c) $I(z)/I(0)$ at $z = 0, 100, 200, 300, 400,$ and $500 \mu\text{m}$ respectively.

We emphasize that the performance of the grazing waveguide is up to the precision of the refractive index difference between the core and cladding. Practically, the change of refractive index can reach an accuracy of 10^{-5} in a germania-doped silica-glass [25].

4. Conclusion

In conclusion, we have introduced a new way of producing a high diffractionless beam based on diminishing the optical phase contrast at the end of a slab waveguide. We were able to generate such grazing mode by virtue of the concept of the adiabatic transition. Therefore, a light sheet produced by the slab waveguide can be beneficial for many optical systems. Furthermore, for beams coming out from the slab waveguide, a lens system is usually employed to collimate light from diffraction. The lens system is either bulky or complicated, which limits the application to micro-systems. On the contrary, the tiny and simple design of the grazing waveguide provides a unique solution that can be directly integrated with other optical instruments. The same concept can apply to an optical fiber. The generation of a diffractionless beam by only one single optical element would be very useful in integrated optics. For example, in bio-imaging application, the light sheet can provide uniform deeper micro-illumination for SPIM.

Acknowledgements

This work was supported in part by NIH grants 1-RO1 EB006432 and U24 CA 092782.

*The author contributed in conceptual development, designing the device and numerical modeling of this work.

^{2,3}These authors contributed equally in supervising this work.